Identification of the open loop dynamics of a bicycle-rider system under manual control

Jason K. Moore and Mont Hubbard

September 27, 2013

1 Introduction

Today's dynamical experiments are capable of delivering a staggering amount of both kinematic and kinetic data from complex dynamical systems. Such a large amount of data lends itself to data driven modeling approaches that can potentially provide more predictive models than first principles models which make use of the traditional building blocks of dynamical models. These data driven models can also give insight into the deficiencies of first principles models. Here we explore the bicycle-rider system with data driven modelling.

The bicycle/motorcycle-rider system has been described with a variety of models, both simple [13] and complex [12]. Many studies of bicycles rely on the benchmarked Whipple model [8], with or without the addition of tire models, for analytical studies of the system and simulation comparisons. The Whipple bicycle model [14] is regarded as a highly predictive, yet "simple", model of the bicycle-rider system and is constructed from first principles, yet very little experimental data proves that the Whipple model is in fact robust at predicting the open loop dynamics of the bicycle-rider system. The benchmarked Whipple bicycle model [8] provides a minimalistic standard base model in a manageable analytic framework capable of describing the essential dynamics such as speed dependent stability, steer and roll coupling, and non-minimum phase behavior.

We are only aware of two significant experimental attempts at validating the Whipple model with data generated from bicycle experiments. The most cited, [7, 6], shows that the Whipple model is predictive of a *riderless* bicycle in a gymnasium and on a treadmill for speeds in its predicted stable speed range, 4-6 m/s. The second, [1], shows that the Whipple model reduced to a linear steady turn can predict the kinematics, but is not so good at predicting the rider's applied steering torque.

It is also worth noting that [3] and [4, 5] have identified the open loop dynamics of the motorcycle-rider system. Eaton used frequency domain identification techniques to identify the dynamics, which are know to be problematic for closed loop identification [**?**]. James showed that identified ARX models with lower order than typical first principles models can predict the measured motion, but does not find very good agreement with his high order first principles models.

In an attempt to validate the Whipple model, we have collected a large set of time history data from an instrumented bicycle ridden under manual control. The measurements include some of the most important kinematic and kinetic variables describing the bicycle-rider motion from three different riders on the same bicycle for a variety of maneuvers and speeds. These experiments generated approximately 1.7 million time samples from each of about 30 sensors sampled at 200 hertz (representing about 2.4 hours of real time).

As pointed out by many, in particular the motorcycle researchers, there is very good reason to question some of assumptions in the Whipple model. The main questionable assumption being knife-edge no side-slip wheels, especially when under a rider's weight. And secondly, the rider's biomechanics have much more influence and coupling to the bicycle than the motorcycle, which must be accounted for. Our identified models attempt to account for these and more descrepancies.

2 Instrumented Bicycle

We developed an instrumented bicycle that had a unique combination of sensors for dynamic measurements that are known to be important indicators of the bicycle-rider system motion. The bicycle's primary design criteria were as follows:

- The bicycle should be sized for our intended riders.
- The rider's biomechanical movement, including pedaling, should be restricted as much as possible so that the Whipple model's rigid rider assumption is more probable.
- The instrumentation should accurately measure the fundamental kinematics of the bicycle: three dimensional rates and orientations of the bicycle rear frame, front frame, and wheels.
- The instrumentation should accurately measure the rider's applied steering torque.
- The instrumentation should accurately measure an applied lateral disturbance force to the bicycle frame.
- The experiments could be performed on open road or on a treadmill.

With these criteria in mind we constructed a bicycle with an electric propulsion system and rigid rider harness and an assortment of sensors, Figure 2. The rear frame three dimensional angular rates and a three dimensional point acceleration were measured with a VectorNav VN-100 inertial measurement unit, the rear frame roll angle was measured with a rotary potentiometer mounted to a small lightweight trailer, the steer angle was measured with a rotary potentiometer, the axial torque in the steer tube by a Futek 150 in-lb (17 Nm) TFF350 torque sensor, the lateral perturbation force by a load cell 100 lb force load cell (Interface SSM-100), the angular rate about the steer axis of the front frame by a rate gyro Single axis rate gyro (Silicon Sensing CRS03-04S), and the rear wheel angular rate by a DC generator. See [9] for full details of the equipment.

3 Experiments

The analysis herein focuses on the two maneuvers which we call *Heading Tracking* and *Lateral Deviation Tracking*. During heading tracking the rider was instructed to simply balance the bicycle and keep a relatively constant heading while focusing their vision at a point in the far distance. During lateral deviation tracking the rider was instructed to focus on a straight line that was marked on the ground and to attempt to keep the front wheel on the line.

Both tasks were performed with and without the application of a manually applied lateral perturbation forces just below the seat. The forces were applied randomly in direction and time during the trials. Each maneuver was performed on both a 1 meter wide treadmill and an open gymnasium floor. See [9] for detailed descriptions of the trials.

4 Data

The physical parameters (geometry, mass, center of mass, and moments of inertia) of both the bicycle and the rider were estimated using the methods in [9] and [15]. The bicycle was measured to get accurate estimates of the parameters used in the benchmark model, [8]. The combined inertial properties of the bicycle rear frame and the rider were computed with standard methods. Two open source software packages, `yeadon` [2] and `BicycleParameters` [10] manage and process the data physical parameter data.

Before each day of testing, base data was collected for the system's sensors for calibration purposes. Then for each trial a set of meta data and raw time series were collected from the bicycle's onboard DAQ system. This data was stored in a HDF5 database for easy querying and

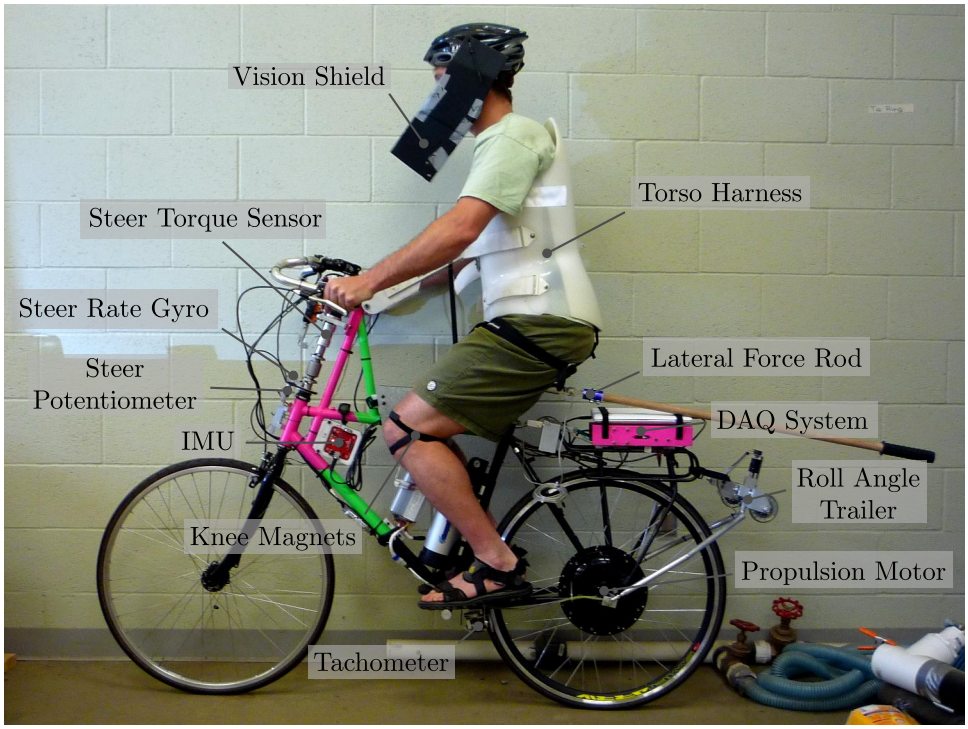

Figure 1: The instrumented bicycle with rider L seated in the harness.

Table 1: The fundamental measurements from the instrumented bicycle.

Variable	Description	Units
v	wheel center speed magnitude	m/s
δ, ϕ, ψ	steer, roll and yaw angles	rad
$\dot{\delta}, \dot{\phi}, \dot{\psi}, \dot{\theta}_B$	steer, roll, yaw, and rear wheel angular rates	rad/s
T_δ, F_{c_l}	steer torque, lateral perturbation force	NM, N

retrieval in the data analysis step. The raw data was then processed to obtain the desired time histories defined by the Whipple model coordinates, described in Table 1.

The signals were measured and processed as described in [9]. The roll and steer accelerations were estimated by numerically differentiating the roll and steer rate signals. Before identification computations we subtracted the means over time of the signals that were generally symmetric about zero, i.e. all but lateral force and speed. Then all of the signals were filtered with a second order low pass Butterworth filter at 15 Hz cutoff frequency.

The experimental data was collected on seven different days and amounted to about 600 individual trials with three different riders. We used 374 of the runs for the following analysis.

5 Identification

The linear Whipple model is a 4th order system with roll angle ϕ, steer angle δ, roll rate $\dot{\phi}$, and steer rate $\dot{\delta}$ selected as the independent states and with roll T_ϕ and steer T_δ torques as the generalized forces and system inputs. In place of the roll torque input, we extend the model to include a lateral force F acting at a point on the frame to provide a new input, accurately modelling imposed lateral perturbations (see [9] for details). We also examine a second candidate model which adds the inertial effects of the rider's arms to the Whipple model, also described in [9]. This model was designed to more accurately account for the fact that the riders were free to move their arms with the front frame of the bicycle. This model is similar in fashion to the upright rider in [11], but with slightly different joint definitions. Constraints are chosen so that no additional degrees of freedom are added, keeping the system both tractable and comparable to the benchmarked Whipple model.

For the identification procedure we make the assumptions that the model is (1) linear, (2) is fourth order, and (3) we can measure the states and inputs directly while the system is under closed loop control by the rider. We then employ the *direct identification* approach to identify the plant.

5.1 Model structure

Identification of the bicycle-rider equations of motion can be formulated with respect to an augmented benchmark canonical form based on [8], shown in Equation 1. If the time varying quantities in the equations are all measured at each time step, the coefficients of the linear equations can be estimated given enough time steps.

$$\mathbf{M}\ddot{q} + v\mathbf{C}_1\dot{q} + [g\mathbf{K}_0 + v^2\mathbf{K}_2]q = T + HF \tag{1}$$

where the time-varying states roll and steer are collected in the vector $q = [\phi \quad \delta]^T$, the time varying inputs roll torque and steer torque are collected in the vector $T = [T_\phi \quad T_\delta]^T$, and $H = [H_{\phi F} \quad H_{\delta F}]^T$ is a vector describing the linear contribution of the lateral force, F, to the roll and steer torque equations. This equation assumes that the speed, v, is constant with respect to time as the model was linearized about a constant speed equilibrium, but we treat v as a time varying parameter because the measured longitudinal acceleration is negligible.

5.2 Identification

A simple analytic identification problem can be formulated from the canonical form. If we have good measurements of q, their first and second derivatives, forward speed v, and the inputs T_δ and F, the entries in $\mathbf{M}$, $\mathbf{C}_1$, $\mathbf{K}_0$, $\mathbf{K}_2$, and H can be identified by forming two simple linear regressions (one for each equation in the canonical form).

The roll and steer equations each can be put into a simple linear form:

$$\mathbf{\Gamma}\Theta = Y \tag{2}$$

where Θ is a vector of the unknown constant matrix entries and the design matrix, $\mathbf{\Gamma}$, and the prediction vector, Y, are made up of the inputs and outputs measured during a run. Θ can be all or a subset of the entries in the canonical matrices and can be estimated using the well known linear least squares solution, Equation 3.

$$\hat{\Theta} = [\mathbf{\Gamma}^T\mathbf{\Gamma}]^{-1}\mathbf{\Gamma}^T Y \tag{3}$$

Equation 3 can be solved for each run individually, a portion of a run, or a set of runs.

Also, all of the parameters in the canonical matrices need not be estimated. The analytical formulation of the Whipple model bicycle model [8] gives a good idea of which entries in the matrices we may be more certain about from our physical parameters measurements. We fixed any parameters which were not a function of trail, front assembly moments and products of inertia, or equal to zero. This is because the true trail is difficult to measure, the inertia of the front frame plays a large roll in the steer dynamics.

For the roll equation this leaves $M_{\phi\delta}$, $C_{1\phi\delta}$, and $K_{0\phi\delta}$ as free parameters, and for the steer equation this leaves $M_{\delta\phi}$, $M_{\delta\delta}$, $C_{1\delta\phi}$, $C_{1\delta\delta}$, $K_{0\delta\phi}$, $K_{0\delta\delta}$, $K_{2\delta\delta}$, and $H_{\delta F}$ as free parameters.

We start by identifying the three coefficients of the roll equation for the given data using

$$\begin{bmatrix} \ddot{\delta}(1) & v(1)\dot{\delta}(1) & g\delta(1) \\ \vdots & \vdots & \vdots \\ \ddot{\delta}(N) & v(N)\dot{\delta}(N) & g\delta(N) \end{bmatrix} \begin{bmatrix} M_{\phi\delta} \\ C_{1\phi\delta} \\ K_{0\phi\delta} \end{bmatrix} \tag{4}$$

$$= \begin{bmatrix} H_{\phi F}F(1) - M_{\phi\phi}\ddot{\phi}(1) - C_{1\phi\phi}v(1)\dot{\phi}(1) - K_{0\phi\phi}g\phi(1) - K_{2\phi\phi}v(1)^2\phi(1) - K_{2\phi\delta}v(1)^2\delta(1) \\ \vdots \\ H_{\phi F}F(N) - M_{\phi\phi}\ddot{\phi}(N) - C_{N\phi\phi}v(N)\dot{\phi}(N) - K_{0\phi\phi}g\phi(N) - K_{2\phi\phi}v(N)^2\phi(N) - K_{2\phi\delta}v(N)^2\delta(N) \end{bmatrix}$$

We then enforce the assumptions that $M_{\phi\delta} = M_{\delta\phi}$ and $K_{0\phi\delta} = K_{0\delta\phi}$ to fix these values in the steer equation to the ones identified in the roll equation, leaving fewer free parameters in the steer equation. Finally, I identify the remaining steer equation coefficients with

$$\begin{bmatrix} \ddot{\delta}(1) & v(1)\dot{\phi}(1) & v(1)\dot{\delta}(1) & g\phi(1) & v(1)^2\delta(1) & -F(1) \\ \vdots & \vdots & \vdots & \vdots & \vdots & \vdots \\ \ddot{\delta}(N) & v(N)\dot{\phi}(N) & v(N)\dot{\delta}(N) & g\phi(N) & v(N)^2\delta(N) & -F(N) \end{bmatrix} \begin{bmatrix} M_{\delta\delta} \\ C_{1\delta\phi} \\ C_{1\delta\delta} \\ K_{0\delta\phi} \\ K_{2\delta\delta} \\ H_{\delta F} \end{bmatrix}$$

$$= \begin{bmatrix} T_\delta(1) - M_{\delta\phi}\ddot{\phi}(1) - K_{0\delta\delta}g\delta(1) - K_{2\delta\phi}v(1)^2\phi(1) \\ \vdots \\ T_\delta(N) - M_{\delta\phi}\ddot{\phi}(N) - K_{0\delta\delta}g\delta(N) - K_{2\delta\phi}v(N)^2\phi(N) \end{bmatrix} \tag{5}$$

6 Results

From our larger pool of data, we selected data for three riders on the same bicycle, performing two maneuvers, in two different environments. There is little reason to believe the dynamics of the open loop system should vary much with respect to different maneuvers, but there is potential variation across riders due to the differences in their inertial and musculoskeletal properties and there may be variation across environments because of the differences in the wheel to floor interaction. We computed the best fit model across a series of runs to benefit from the large dataset. We then selected four scenarios with a total of 12 different models:

- All riders in both environments, one data set

Table 2: The VAF in the roll equation computed for each subset of data (rows) and each model (columns).

	A-A	A-H	A-P	C-A	C-H	C-P	J-A	J-H	J-P	L-A	L-H	L-P	Whipple
C-H	29.3%	29.6%	25.5%	30.5%	30.9%	29.6%	28.4%	28.2%	23.4%	27.8%	29.8%	18.1%	5.0%
C-P	18.3%	17.8%	17.6%	19.1%	18.6%	19.2%	17.6%	17.1%	16.4%	18.0%	17.8%	14.8%	8.7%
C-A	21.7%	21.4%	20.1%	22.7%	22.4%	22.5%	21.0%	20.5%	18.7%	21.1%	21.5%	15.9%	7.5%
J-H	30.5%	31.1%	27.0%	28.9%	29.5%	27.9%	30.8%	31.2%	26.1%	29.7%	30.3%	21.4%	-0.4%
J-P	47.6%	44.4%	50.0%	43.7%	43.0%	43.7%	47.6%	44.5%	50.5%	48.9%	41.3%	49.4%	36.1%
J-A	35.6%	35.1%	33.6%	33.4%	33.6%	32.6%	35.8%	35.3%	33.1%	35.3%	33.7%	29.3%	9.9%
L-H	25.5%	26.9%	20.1%	25.9%	26.5%	24.7%	25.1%	26.4%	18.2%	23.8%	27.4%	12.4%	-5.5%
L-P	47.2%	43.5%	51.6%	43.4%	41.8%	44.5%	47.2%	44.3%	52.2%	49.3%	40.2%	53.3%	48.5%
L-A	37.8%	36.5%	37.4%	36.0%	35.4%	36.0%	37.6%	36.6%	36.7%	38.1%	34.9%	34.2%	22.7%
A-H	29.6%	30.2%	25.7%	28.7%	29.3%	27.7%	29.5%	30.0%	24.4%	28.5%	29.8%	19.5%	2.8%
A-P	34.9%	33.0%	36.2%	33.4%	32.6%	33.7%	34.6%	32.8%	36.0%	35.7%	31.3%	35.0%	27.4%
A-A	32.1%	31.5%	30.5%	30.9%	30.8%	30.4%	31.9%	31.3%	29.6%	31.8%	30.5%	26.4%	13.6%

Table 3: The VAF in the steer equation computed for each subset of data (rows) and each model (columns).

	A-A	A-H	A-P	C-A	C-H	C-P	J-A	J-H	J-P	L-A	L-H	L-P	Whipple
C-H	58.3%	60.8%	49.4%	53.1%	59.1%	38.4%	60.8%	59.0%	56.8%	50.6%	53.5%	42.3%	61.4%
C-P	48.5%	50.7%	45.0%	44.4%	46.1%	39.8%	52.0%	51.3%	49.0%	41.8%	42.9%	38.3%	52.7%
C-A	52.9%	55.3%	47.1%	48.4%	51.9%	39.1%	56.0%	54.9%	52.6%	45.8%	47.7%	40.2%	56.7%
J-H	70.2%	69.9%	62.9%	66.0%	70.0%	50.2%	68.9%	66.8%	68.2%	66.2%	67.5%	58.5%	68.7%
J-P	72.3%	70.3%	71.6%	69.2%	65.6%	65.4%	71.0%	67.6%	73.5%	70.7%	68.5%	67.8%	68.1%
J-A	70.7%	70.0%	65.0%	66.8%	68.8%	53.8%	69.4%	67.0%	69.6%	67.4%	67.8%	60.7%	68.5%
L-H	67.8%	68.5%	58.7%	61.9%	67.2%	43.6%	67.6%	65.2%	66.4%	62.3%	63.7%	53.6%	67.0%
L-P	72.6%	70.6%	73.7%	68.9%	66.5%	62.9%	72.7%	68.3%	77.3%	68.9%	63.7%	69.1%	68.6%
L-A	70.1%	69.5%	65.3%	65.2%	66.8%	52.1%	70.0%	66.7%	71.2%	65.4%	63.7%	60.4%	67.7%
A-H	68.0%	68.4%	60.2%	63.4%	67.9%	47.4%	67.5%	65.4%	66.2%	63.2%	64.8%	55.2%	66.8%
A-P	64.8%	64.4%	63.5%	61.4%	60.0%	56.9%	65.6%	63.0%	66.4%	60.9%	59.3%	58.6%	63.1%
A-A	66.8%	66.9%	61.3%	62.7%	64.9%	50.6%	66.8%	64.5%	66.3%	62.4%	62.7%	56.4%	65.5%

- All riders in each environment, two data sets
- Each rider in both environments, three data sets
- Each rider in each environment, six data sets

6.1 Model Quality

The predictive capability and quality of a given model can be quantified by an assortment of criteria and methods. We used two criteria to judge the quality of the identified models with respect to the available data: (1) we compute the variance accounted for (VAF) (i.e. coefficent of determination) with respect to the linear least squares solution for each set of run and each identified model and (2) simulate the identified model given the measured steer torque and lateral force for each run and compute VAF with respect to the four predicted outputs and measured outputs.

The second method works well when the open loop system is stable, but if it is unstable as is so in the case of this bicycle, it may be difficult to simulate. Searching for initial conditions that give rise to a stable model for the duration of the run or simulating by weighting the future error less may relieve the instability issues. We chose the former method for these computations.

For method (1) the *variance accounted for* (VAF) by the model for both the roll torque and the steer torque equations are

$$\mathrm{VAF}_{\phi,\delta} = 1 - \frac{||\mathbf{\Gamma}_{\phi,\delta}\hat{\Theta}_{\phi,\delta} - Y_{\phi,\delta}||}{||Y_{\phi,\delta} - \bar{Y}_{\phi,\delta}||} \tag{6}$$

where $\bar{Y}$ is the mean of Y.

We compute the two VAF values for each of the subsets of data from the 12 scenario combinations using 13 models: the 12 identified models and the Whipple model. The columns in tables 2 and 3 correspond to the models and the rows correspond to the data subsets the VAF was computed with. The maximum VAF in a row gives an indication of the best model for predicting that set of runs.

Tables 2 and 3 lead to these observations:

Table 4: The median VAF of each output variable over 374 runs for each model and the mean of the median VAFs.

	ϕ	δ	$\dot{\phi}$	$\dot{\delta}$	Mean
A-A	28.6%	61.8%	51.8%	65.2%	51.8%
C-H	18.6%	57.2%	52.6%	62.2%	47.7%
L-A	29.4%	59.8%	52.9%	67.9%	52.5%
A-H	24.1%	57.4%	43.1%	64.2%	47.2%
C-A	14.9%	54.5%	51.7%	59.8%	45.2%
J-P	-3.4%	35.4%	34.1%	61.7%	31.9%
L-H	24.3%	57.7%	46.1%	65.7%	48.5%
A-P	29.7%	58.9%	60.6%	63.2%	53.1%
J-H	22.8%	53.6%	42.0%	62.8%	45.3%
L-P	38.2%	62.8%	60.9%	68.4%	57.6%
C-P	19.0%	46.0%	42.0%	47.1%	38.5%
J-A	27.9%	61.0%	49.4%	65.9%	51.1%
Whipple	-21.0%	10.3%	5.8%	12.2%	1.8%
Arm	-33.1%	19.6%	29.7%	33.1%	12.3%

- The models predict the steer torque better than the roll torque.
- The Whipple model is generally poor at predicting the roll torque equation.
- The Whipple model is good at predicting the steer torque.

For method (2), we simulate all 14 models with the inputs measured from the 374 runs and compute the VAF explained by the model for each of the four outputs. Since the models are typically unstable at all of the speeds we tested, we searched for the set of initial conditions which minimizes the VAF for all outputs and ignored any runs in which suitable initial confiditions couldn't be found. Table 6.1 presents the median percent variance accounted for across all runs for the outputs of each model. Based on the mean VAF across the outputs for each model the best model seems to be L-P. Notice that the Whipple model is the poorest predictor and the arm model is the second poorest.

The following are observed from Table 6.1:

- For all outputs other than roll angle, the arm model is better than the Whipple model.
- All of the identified models are better predictors than the first principles models.
- Model J-P has the best average predicitive ability for all of the runs.

6.2 Most predictive model

This section details the characteristics for the identified model which best predicts *all* of the data, the L-P model.

The eigenvalues as a function of speed of the identified model can be compared to those of the Whipple and arm models. Figure 6.2 shows the root locus of the three models as a function of speed. The oscillatory weave mode exists in all three models, stable at all speeds in the arm model but unstable at lower speeds in the other two models. The identified model's oscillatory weave mode is unstable over most of the shown speed range. Above 3 m/s or so, the Whipple model's oscillatory weave mode diverges from the identified model to different asymptotes. The arm model weave mode diverges somewhere in between but shares similar pole locations with the Whipple model at higher speeds. Note that the arm model has an unstable real mode for all speeds.

Figure 6.2 gives a different view of the root locus allowing one to more easily compare the real and imaginary parts of the eigenvalues independently. The imaginary parts of the weave mode

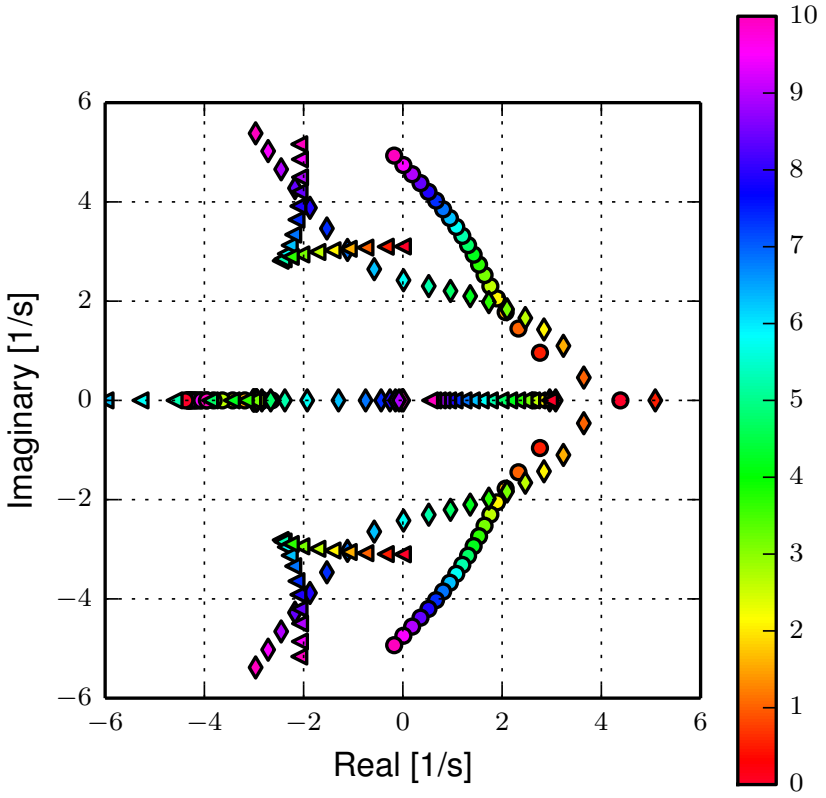

Figure 2: Root locus of the identified model (circle), the Whipple model (diamond), and the arm model (triangle) with respect to speed in m/s.

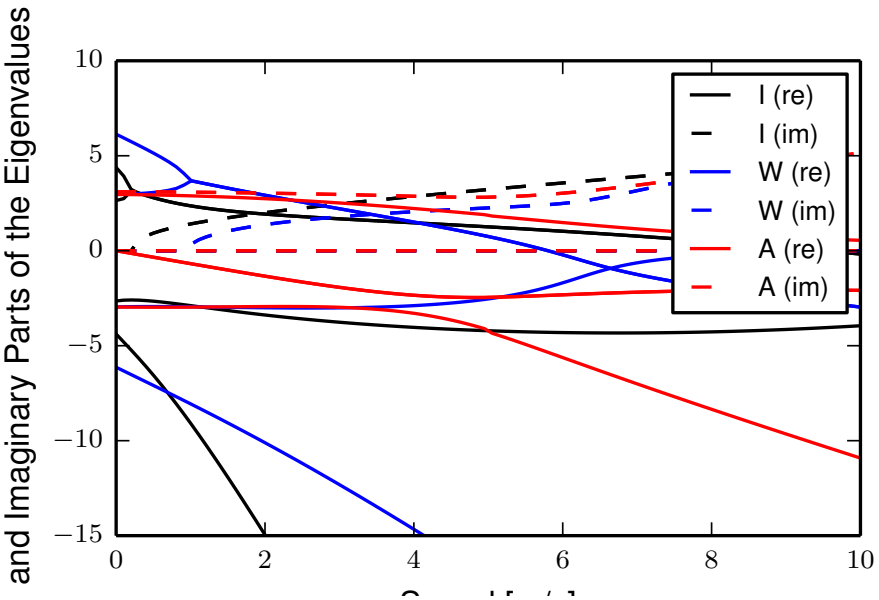

Figure 3: Real and imaginary parts of the eigenvalues as a function of speed for model (I)dentified from all runs, the (W)hipple model and the (A)rm model.

Table 5: The identified $\mathbf{M}$, $\mathbf{C}_1$, $\mathbf{K}_0$, $\mathbf{K}_2$, and H matrices of the L-P model compared to the Whipple Model.

Model	$\mathbf{M}$	$\mathbf{C}_1$	$\mathbf{K}_0$	$\mathbf{K}_2$	H
Whipple	$\begin{bmatrix} 129.362 & 2.260 \\ 2.260 & 0.219 \end{bmatrix}$	$\begin{bmatrix} 0.000 & 41.622 \\ -0.315 & 1.376 \end{bmatrix}$	$\begin{bmatrix} -115.707 & -2.361 \\ -2.361 & -0.737 \end{bmatrix}$	$\begin{bmatrix} 0.000 & 103.943 \\ 0.000 & 2.190 \end{bmatrix}$	$\begin{bmatrix} 0.902 \\ 0.011 \end{bmatrix}$
L-P	$\begin{bmatrix} 129.362 & 2.559 \\ 2.559 & 0.250 \end{bmatrix}$	$\begin{bmatrix} 0.000 & 33.526 \\ -0.549 & 2.100 \end{bmatrix}$	$\begin{bmatrix} -115.707 & -4.526 \\ -4.526 & -0.489 \end{bmatrix}$	$\begin{bmatrix} 0.000 & 103.943 \\ 0.000 & 2.603 \end{bmatrix}$	$\begin{bmatrix} 0.902 \\ 0.011 \end{bmatrix}$

have similar curvature with respect to speed for all the models about 2m/s or so. The identified model has a stable speed range where the Whipple model under predicts the its weave critical speed by almost 3 m/s. The identified caster mode is much faster than the one predicted by the Whipple model which is somewhat counterintuitive because tire scrub torques would probably tend to slow the caster mode. Although, the pneumatic trail and the rider's arm inertia could play a larger role that expected.

The frequency band from 1 rad/s to 12 rad/s is of most concern as it bounds a reasonable range that the human may be able to operate within. The steer torque to roll angle transfer function, Figure 6.2 may be the most important to model accurately as it is the primary method of controlling the bicycle's direction, i.e. commanding roll allows one to command yaw. At 2 m/s the magnitude is similar for all three models. At 4 m/s the identified model has a larger gain than the first principles models. In fact, the identified model seems to vary little with speed, which contrasts the stronger speed dependence of the first principles models. The low frequency behavior of the identified model is not well predicted by the Whipple and arm models at the three highest speeds but about about 3 rad/s the arm model shows better magnitude matches than the Whipple model.

Table 6.2 gives the values of the identified coefficients to the roll and steer equations for the L-P model.

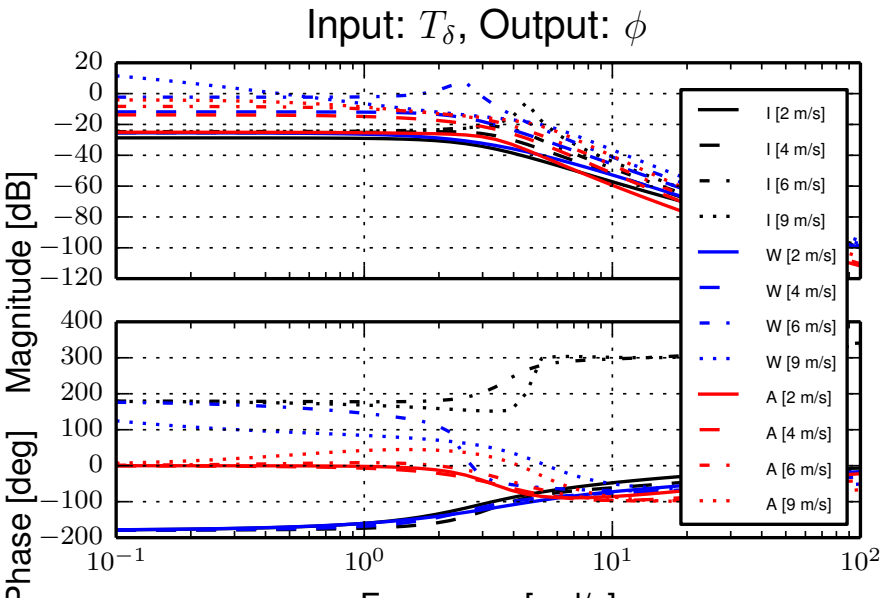

Figure 4: Frequency response of the three models, (I)dentified, (W)hipple, and (A)rm, at four speeds (2, 4, 6, and 9 m/s). The color indicates the model and the line type indicates the speed

7 Discussion

We have shown that a fourth order linear model is adequate for describing the motion of the bicycle under manual control in a speed range from approximately 1.5 m/s to 9 m/s. Results from this study show that higher order models may not be necessary for predicting the bicycle-rider plant dynamics. This is an important finding, as many researchers develop models using first principles which have orders much greater than 4, with degrees of freedom associated with tire slip, frame flexibilities, and rider biomechanics, which may be overkill for many prediction purposes. But, results also reveal that fourth order archetypal first principles models are not predictive enough to fully describe the dynamics. These deficiencies are most likely due to un-modeled effects, with knife-edge, no side-slip wheel contact assumptions being the most probable candidate. Un-modeled rider biomechanics such as passive arm stiffness and damping and head motion may play a role too. It is likely that something as simple as a "static" tire scrub torque is needed to improve the fidelity of the Whipple first principles derivations, but that doesn't preclude that the addition of a tire slip model, adding more degrees of freedom, might also improve the predictive ability.

Acknowledgements

This paper is based on work supported by the National Science Foundation under Grant No 0928339. Karl Åström gave me the ideas for the canonical form.

References

[1] Stephen M. Cain and Noel C. Perkins. Comparison of experimental data to a model for bicycle steady-state turning. *Vehicle System Dynamics*, 50(8):1341–1364, 2012.

[2] Christopher Dembia. *Yeadon: A Python Library For Human Inertia Estimation*, 2011. http://pypi.python.org/pypi/yeadon/.

[3] David J. Eaton. *Man-Machine Dynamics in the Stabilization of Single-Track Vehicles*. PhD thesis, University of Michigan, 1973.

[4] Stephen R. James. Lateral dynamics of an offroad motorcycle by system identification. *Vehicle System Dynamics*, 38(1):1–22, July 2002.

[5] Stephen R James. Lateral dynamics of motorcycles towing single-wheeled trailers. *Vehicle System Dynamics: International Journal of Vehicle Mechanics and Mobility*, 43(8):581–599, 2005.

[6] J. D. G. Kooijman and A. L. Schwab. Experimental validation of the lateral dynamics of a bicycle on a treadmill. In *Proceedings of the ASME 2009 International Design Engineering Technical Conferences & Computers and Information in Engineering Conference, IDETC/CIE 2009*, number DETC2009-86965, 2009.

[7] J. D. G. Kooijman, A. L. Schwab, and J. P. Meijaard. Experimental validation of a model of an uncontrolled bicycle. *Multibody System Dynamics*, 19:115–132, May 2008.

[8] J. P. Meijaard, Jim M. Papadopoulos, Andy Ruina, and A. L. Schwab. Linearized dynamics equations for the balance and steer of a bicycle: A benchmark and review. *Proceedings of the Royal Society A: Mathematical, Physical and Engineering Sciences*, 463(2084):1955–1982, August 2007.

[9] Jason K. Moore. *Human Control of a Bicycle*. PhD thesis, University of California, Davis, Davis, CA, August 2012.

[10] Jason K. Moore, J. D. G. Kooijman, A. L. Schwab, and Mont Hubbard. Rider motion identification during normal bicycling by means of principal component analysis. *Multibody System Dynamics*, 25:225–244, 2011.

[11] A. L. Schwab and J. D. G. Kooijman. Lateral dynamics of a bicycle with passive rider model. In *The 1st Joint International Conference on Multibody System Dynamics*, Lappeenranta, Finland, May 2010.

[12] Robin S. Sharp. Stability and control of motorcycles. *Journal of Mechanical Engineering Science*, 13(5):316–329, 1971.

[13] S. Timoshenko and D. H Young. *Advanced dynamics*. McGraw-Hill, New York, 1948.

[14] Francis J. W. Whipple. The stability of the motion of a bicycle. *Quarterly Journal of Pure and Applied Mathematics*, 30:312–348, 1899.

[15] M. R. Yeadon. The simulation of aerial movement–i. the determination of orientation angles from film data. *Journal of Biomechanics*, 23(1):59 – 66, 1990.